Drought losses in China might double between the 1.5 °C and 2.0 °C warming

Buda Su[a,b,c,1], Jinlong Huang[a,d,1], Thomas Fischer[c,e], Yanjun Wang[b], Zbigniew W. Kundzewicz[f,g,2], Jianqing Zhai[b,c], Hemin Sun[b], Anqian Wang[a,d], Xiaofan Zeng[h], Guojie Wang[b], Hui Tao[a], Marco Gemmer[c,e], Xiucang Li[b,c], and Tong Jiang[b,c,2]

[a]State Key Laboratory of Desert and Oasis Ecology, Xinjiang Institute of Ecology and Geography, Chinese Academy of Sciences, Urumqi 830011, China; [b]Collaborative Innovation Center on Forecast and Evaluation of Meteorological Disaster, School of Geographic Sciences, Nanjing University of Information Science & Technology, Nanjing 210044, China; [c]National Climate Center, China Meteorological Administration, Beijing 100081, China; [d]University of Chinese Academy of Sciences, Beijing 100049, China; [e]Department of Geosciences, Eberhard Karls University, 72074 Tübingen, Germany; [f]Institute for Agricultural and Forest Environment, Polish Academy of Sciences, 60809 Poznan, Poland; [g]Potsdam Institute for Climate Impact Research, 14473 Potsdam, Germany; and [h]School of Hydropower & Information Engineering, Huazhong University of Science and Technology, Wuhan 430074, China

Edited by Amir AghaKouchak, University of California, Irvine, CA, and accepted by Editorial Board Member Gregory P. Asner August 16, 2018 (received for review February 8, 2018)

We project drought losses in China under global temperature increase of 1.5 °C and 2.0 °C, based on the Standardized Precipitation Evapotranspiration Index (SPEI) and the Palmer Drought Severity Index (PDSI), a cluster analysis method, and "intensity-loss rate" function. In contrast to earlier studies, to project the drought losses, we predict the regional gross domestic product under shared socioeconomic pathways instead of using a static socioeconomic scenario. We identify increasing precipitation and evapotranspiration pattern for the 1.5 °C and 2.0 °C global warming above the preindustrial at 2020–2039 and 2040–2059, respectively. With increasing drought intensity and areal coverage across China, drought losses will soar. The estimated loss in a sustainable development pathway at the 1.5 °C warming level increases 10-fold in comparison with the reference period 1986–2005 and nearly threefold relative to the interval 2006–2015. However, limiting the temperature increase to 1.5 °C can reduce the annual drought losses in China by several tens of billions of US dollars, compared with the 2.0 °C warming.

drought | drought losses | projections | global warming | China

Droughts are major weather-driven natural disasters that encompass large areas. Droughts can occur everywhere, including water-rich areas, due to occasional anomalies in climatic variables. The impacts of drought events with similar intensity and duration can largely vary, depending on socioeconomic and environmental characteristics of the affected regions. Around the world, drought losses have significantly increased in recent years, for a range of reasons, including nonclimatic factors (1, 2). Enhanced drying has been observed and projected over many land areas under warming climate, due to increasing atmospheric concentrations of greenhouse gases (3–5). The direction of observed increase in global aridity is consistent with model-based projections (3). Since 2010, frequent and severe drought events in southern China, a region considered to be humid, have been given much attention and have resulted in national enhancement of drought research. Previous studies reported that significant dryness trends detected in the transitional belt of humid and arid climate regions in China for the last half-century and the reduction in regional precipitation play a major role in a changing pattern of drought intensity and duration (6–8).

With expected increases in severe and widespread drought events in the 21st century (3, 9) and further strong growth in the gross domestic product (GDP), more assets will be exposed to the impacts of droughts, which will eventually lead to higher drought losses in the future. To reduce the risk and impacts of a warming climate, the Paris Agreement proposes to hold the increase in global mean temperature to well below 2.0 °C above preindustrial levels and to pursue efforts to limit the warming to 1.5 °C (10). Most projections agree that the warming rate of China will be faster than the global mean (11) and the country might be seriously threatened by global warming-induced disasters. Existing studies in China focus mainly on projections of drought characteristics, with the estimation of drought losses being largely determined by changes in the physical drought parameters. To date, the inclusion of different shared socioeconomic pathways (SSPs; ref. 12) into a multiscenario approach of loss estimation has not been applied for drought projections over China. Hence, in our study, we project future drought losses in China by applying an approach consisting of multimodel scenario-comparison analyses and event-based loss estimation using two drought indices, namely the Standardized Precipitation Evapotranspiration Index (SPEI) and the Palmer Drought Severity Index (PDSI).

Projected Changes in Dryness Patterns

In this study, future characteristics of climate change impacts are analyzed using 22 ensemble runs from 13 global climate models (GCMs) in CMIP5 (Coupled Model Intercomparison Project phase 5): GFDL-ESM2M, HadGEM2-ES, IPSL-CM5A-LR, MIROC-ESM-CHEM, NorESM1-M, CNRM-CM5, CanESM2,

Significance

We project drought losses in China under global warming of 1.5 °C and 2.0 °C. To assess future drought losses, we project the regional gross domestic product under shared socioeconomic pathways instead of using a static socioeconomic scenario. We identify increasing precipitation and evapotranspiration patterns. With increasing drought intensity and areal coverage across China, drought losses will increase considerably. The estimated losses in a sustainable development pathway at 1.5 °C warming will be 10 times higher than in the reference period 1986–2005 and three times higher than in 2006–2015. Yet, climate change mitigation, limiting the temperature increase to 1.5 °C, can considerably reduce the annual drought losses in China, compared with 2.0 °C warming.

Author contributions: Z.W.K. and T.J. designed research; B.S., J.H., X.Z., and H.T. performed research; B.S., J.H., Y.W., J.Z., H.S., A.W., G.W., and X.L. analyzed data; and B.S., J.H., T.F., Y.W., Z.W.K., J.Z., H.S., A.W., X.Z., G.W., H.T., M.G., X.L., and T.J. wrote the paper.

The authors declare no conflict of interest.

This article is a PNAS Direct Submission. A.A. is a guest editor invited by the Editorial Board.

[1]B.S. and J.H. contributed equally to this work.

[2]To whom correspondence may be addressed. Email: kundzewicz@yahoo.com or jiangtong@cma.gov.cn.

This article contains supporting information online at www.pnas.org/lookup/suppl/doi:10.1073/pnas.1802129115/-/DCSupplemental.

Published online October 1, 2018.

GFDL-CM3, GFDL-ESM2G, IPSL-CM5A-MR, MIROC-ESM, MIROC5, and MRI-CGCM3. Two representative concentration pathways (RCPs) are considered, i.e., RCP2.6 and RCP4.5, which are the most appropriate scenarios for the Paris Agreement's target of keeping the global warming below 1.5 °C or 2.0 °C compared with preindustrial times. Global surface mean temperature in 1986–2005 was 0.61 °C warmer than the preindustrial levels (11), and further increase of 0.89 °C or 1.39 °C, respectively, indicates global warming by 1.5 °C or 2.0 °C. Using a multimodel median, projections for 20-y intervals were estimated when the average global warming reaches the 1.5 °C and 2.0 °C thresholds, respectively, under RCP2.6 and RCP4.5. It is estimated that the 1.5 °C warming threshold would be reached in 2020–2039 under RCP2.6 and the 2.0 °C in 2040–2059 under RCP4.5 (13).

The models project tendencies of precipitation increase for both the 1.5 °C and 2.0 °C global warming levels in the whole of China, with higher model agreement at the northern regions (Fig. 1 *A* and *E*). The increasing trend is agreed by more than 66% of GCM runs for 80% and 96% of grids over China at the 1.5 °C and 2.0 °C warming, respectively. Considerably more significant precipitation increases are projected for the period 2040–2059, demonstrating a positive correlation between precipitation and temperature for the next decades.

Significant increases in potential evapotranspiration are projected throughout China for both target periods (Fig. 1 *B* and *F*). The positive changes in evapotranspiration are more significant for the 2.0 °C warming period of 2040–2059, in the parts of North, Northwest, and Southwest China than those at the 1.5 °C warming. Compared with precipitation, evapotranspiration increase is more obvious in southern China as a whole. The increasing trend is consistent for most GCM runs for 85% and 98% of grid cells over China at the 1.5 °C and 2.0 °C warming scenarios, respectively.

Drought conditions can be assessed from different meteorological, hydrological, and socioeconomic aspects, so that decision on the choice of drought indices is needed (14–16). A simple and commonly used index, the Standardized Precipitation Index (SPI), allows the direct comparison of precipitation anomalies among different climatic regions. Nevertheless, it is widely acknowledged that evapotranspiration plays a major role in the generation of droughts in the warmer world (4, 17). Hence, two other drought indices are used to address the long-term characteristics of dryness and wetness in current study. The SPEI (cf. refs. 18 and 19) takes precipitation, temperature, and evapotranspiration into account and thus represents a simple climatic water balance. The PDSI (cf. refs. 20 and 21) takes precipitation, evapotranspiration, and available water storage capacity as input to compute a water balance for area of interest.

With regard to the reference period, dryness in most of southern China is identified consistently by both the SPEI and the PDSI indices in the warming climate. According to SPEI, large areas in Northeast and North, some parts of East, Central, and Southwest China might be in wetter conditions, but vast areas of western and southern China will be drier at the 1.5 °C warming level. Percentages of area getting wetter and drier will be about 39% and 61%, and the changes are significant at 7% and 36% of the entire territory of China. Nearly 75% of the area of China will be getting drier and, for 51% of the area, change is projected to be significant at the 2.0 °C, whereas wetter conditions will be in Northeast, small fractions of North, Northwest, Southwest, and East China (Fig. 1 *C* and *G*). A comparatively weaker drying trend is estimated by PDSI, which shows significant wetness in large parts of northern China, except for parts of Northwest and Northeast regions. Meanwhile, at least 66% of GCMs at both the 1.5 °C and 2.0 °C warming agree on significant increase of dryness conditions projected by PDSI in southern China. About 40% and 37% of the country area are projected to

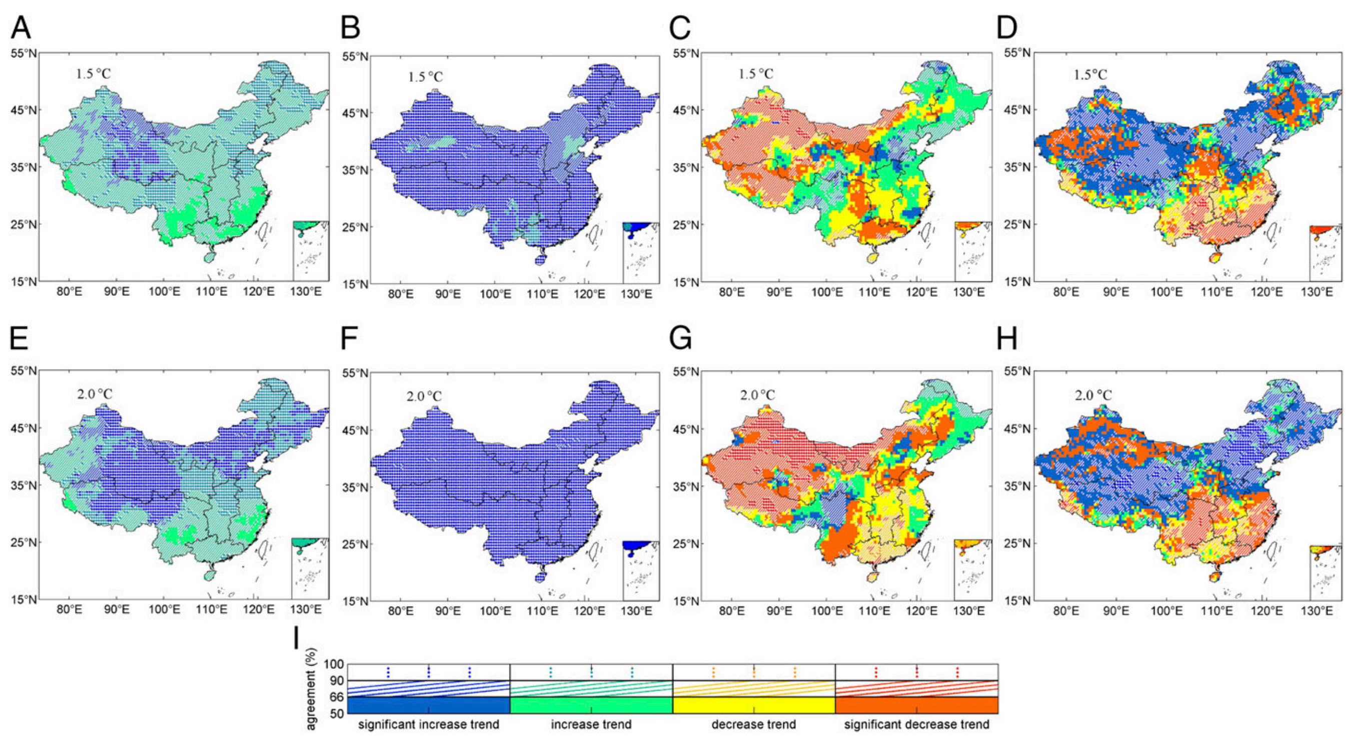

Fig. 1. Projected changes in precipitation (*A* and *E*), potential evapotranspiration (*B* and *F*), drought conditions of the SPEI (*C* and *G*), and the PDSI (*D* and *H*) by multimodel median for the 1.5 °C and 2.0 °C warming scenarios (corresponding to periods of 2020–2039 and 2040–2059, respectively) relative to the reference period (1986–2005) over China. The significance of the changes was tested with the two-sample *t* test at the 0.05 significance level. The similarity among the 22 GCM runs is given for the 90~100% and 66~90% (/) agreement level. Polygons denote subregions (defined in *SI Appendix*, Fig. S1) in China.

get drier, with a significant decrease at 25% and 27% of the area for the 1.5 °C and the 2.0 °C, respectively (Fig. 1 *D* and *H*).

Projection of Droughts

A spatial-temporal drought event is usually characterized by its duration, intensity, and contiguous areal coverage (8, 22, 23). In this study, we define a drought event as occurring if the SPEI ≤ −1 (or the PDSI ≤ −2) at the area exceeding 50,000 km^2 (*SI Appendix*, Table S4), because events with such thresholds usually lead to considerable economic losses (24).

For the period of 1986–2005, average intensities of GCM-simulated drought events over China as deduced by the SPEI and PDSI fluctuate around −1.83 and −3.6, respectively, indicating severe dryness. Higher intensities are projected with the climate warming. The average drought intensity, determined by the SPEI, will further increase to −2.10 and −2.25 at the 1.5 °C and the 2.0 °C warming level, respectively, and that by the PDSI, will reach −4.0 and −4.2, indicating extremely dry conditions. Large-area droughts with more than 2 million km^2 coverage are projected to have slightly lower average intensities than small-area droughts (Fig. 2 *A* and *C*).

Along with intensities, contiguous area of drought events for both warming levels will also increase. The average drought event area for the SPEI index criterion is ∼608,300 km^2 for the reference period, projected to increase to 709,400 km^2 and 880,800 km^2 for the 1.5 °C and the 2.0 °C warming, respectively, i.e., an increase of 16.6% and 44.8%. Meanwhile, increase in average drought coverage from 475,900 km^2 for the reference period to 486,500 km^2 and 518,200 km^2 by a rate of 2.2% and 8.9% is estimated for the PDSI index, for the 1.5 °C and the 2.0 °C level, respectively (Fig. 2 *B* and *E*).

In contrast, total frequency of drought events is projected to increase slightly for both the 1.5 °C and 2.0 °C warming scenarios, compared with the reference period. Small-area droughts are projected to decrease in frequency, but larger drought events with an area greater than 500,000 km^2 will likely occur more frequently for the SPEI index. However, for the PDSI index, frequencies of drought events with different coverage are all projected to increase (Fig. 2 *C* and *F*).

Spatially, as indicated by SPEI, drought frequency for the 1.5 °C warming level is projected to decrease slightly in Northeast and Central China. The decreasing trend extends into the 2.0 °C warming level in the Northeast region, while drought frequency increases in most other regions. As for the contiguous drought area, all regions show persistent increasing trends in the future, with the strongest increase in Northwest China, followed by North, Northeast, and South China. Drought intensities also increase consistently in all regions until 2040–2059, while a stronger increase is projected in Northwest, North, East, and Southwest China. According to the PDSI, regions with increased drought frequency are mainly found in Northeast, East, and Southwest China, and increased drought areas are projected to occur in East, South, and Northwest China in the warming climate. To sum up, it was projected that droughts would be more intense throughout China with increased occurrence in East and Southwest regions and larger areal coverage in East, South, and Northwest regions under the warming scenarios, relative to the reference period for both the SPEI and PDSI, but drought severity is projected to be greater for SPEI (Fig. 3).

Event-Based Estimation of Drought Losses

Assumption of a fixed population or an economic status for a historical period is usually made to study the future impacts of a changing climate (25). However, an adequate assessment of climate change impacts must take future socioeconomic development into account, as the economy and the population will be exposed to increasing risk of climate disasters. To this end, five shared socioeconomic pathways (SSPs) have been projected to represent different climate change strategies for mitigation and adaptation. The SSPs include a sustainable world (SSP1), a pathway of continuing historical trends (SSP2), a strongly fragmented world (SSP3), a highly unequal world (SSP4), and a growth-oriented world (SSP5) (26). Among combinations of different greenhouse gas concentration trajectories and socioeconomic pathways, some SSP-RCP combinations are unlikely to occur, e.g., SSP3-RCP2.6 and SSP1-RCP8.5 (27). Considering the socioeconomic challenges to mitigation by different development roads, the RCP2.6 scenario is associated with SSP1 and SSP4, while the RCP4.5 scenario is associated with the other three SSPs (SSP2, SSP3, SSP5).

For the reference period of 1986–2005, average annual drought losses in China amounted to about 4.2 billion US dollars (USD), or 0.23% of the national GDP (*SI Appendix*, Table S6). With the accelerated increase of GDP and improved adaptation capacity,

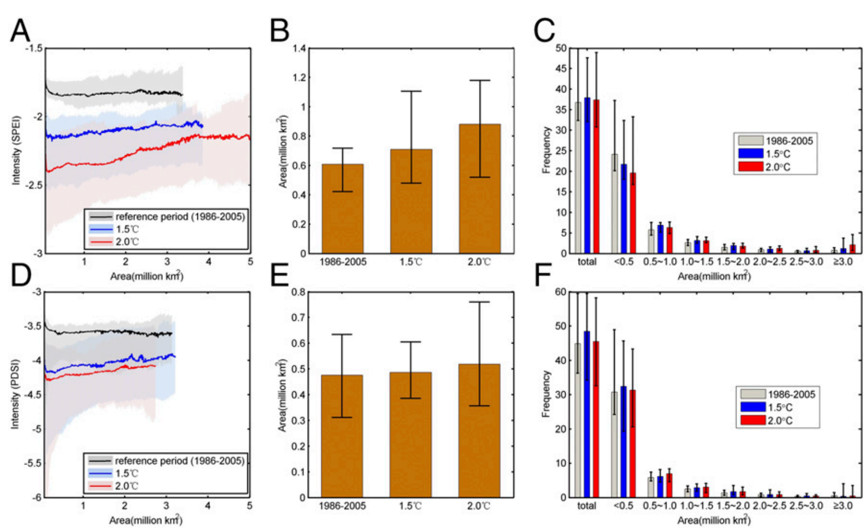

Fig. 2. Averaged drought intensity at different contiguous drought areas (*A* and *D*), averaged coverage of drought events (*B* and *E*), and annual frequency of drought events with different coverage (*C* and *F*) in China for the 1.5 °C and 2.0 °C global warming period and the reference period (1986–2005). Drought characteristics in *A*–*C* and *D*–*F* are deduced by the SPEI and PDSI, respectively. Shadows and lines in *A* and *D* are the bands and median, respectively, for 22 GCM runs. Histograms and black vertical lines in *B* and *C* and *E* and *F* denote the median and range of multimodel projections, respectively.

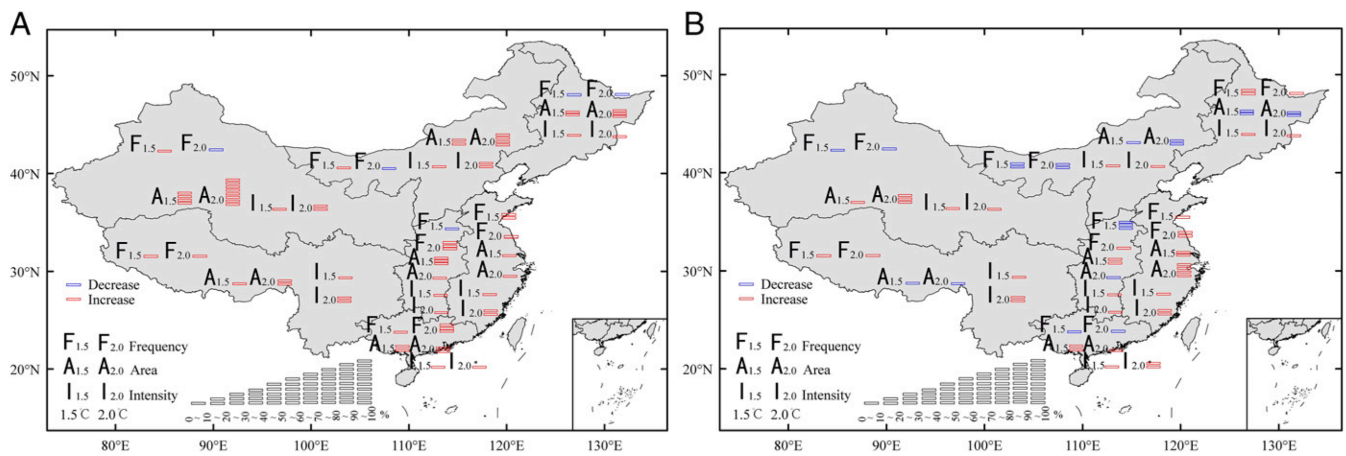

Fig. 3. Percentage change of annual frequency, areal coverage, and intensity of drought events resulting from multimodel median for two levels of global warming (1.5 °C and 2.0 °C), in comparison with the reference period (1986–2005) in seven subregions in China as indicated by the SPEI (*A*) and the PDSI (*B*), respectively.

the share of drought losses to GDP decreased to 0.16% in 2006–2015 with a minimum of 0.04% in 2012 (24). Future drought losses are assessed based on the projected drought intensity by the GCM simulations, the estimated socioeconomic exposure under SSPs, and the "intensity-loss rate" curve changing with time. For setting up intensity-loss rate curve, the relationship between the percent of annual recorded direct economic losses on GDP exposed to drought events and the historical annual average intensity of drought events was established first, and was developed further, to reflect improvements in adaptation capacity in the future (*SI Appendix*, Figs. S8–S10).

Multimodel scenario-comparison analyses show that projected drought losses in a warming climate in China will be higher than those in the reference period, 1986–2005, and in the more recent interval, 2006–2015, with 44 combined results from the 22 GCMs and the two drought indices showing the same direction of change (Fig. 4*A*). A strong agreement from at least 30 results of 44 combinations for all SSPs indicate exceeding of the share of drought losses on GDP in the warming scenarios than that of the current status with higher probability (Fig. 4*B*).

In a sustainable world with effective mitigation and adaptation (SSP1) and with the global warming limited to 1.5 °C, drought-induced economic losses might reach ∼47 billion USD per year by median of 44 estimations from 22 GCM runs and two drought indices, with 95% confidence interval of 44–55 billion (Fig. 4*A*). This projected annual loss is about 10 times higher than for the reference period, while the increase in population and exposed economic assets is included. Taking this into account, the relation of losses to the projected national GDP seems useful. Accordingly, the projected annual average loss for a sustainable world (SSP1) at 1.5 °C warming is about 0.19% of the projected national GDP, lower than that for the reference period of 1986–2005 (Fig. 4*B*). In a highly unequal world of SSP4, not much difference is projected for GDP development in China before the mid-21st century (*SI Appendix*, Fig. S7), estimated annual drought loss will only be slightly lower than for a sustainable world with absolute value of 46 [95% confidence interval: 43–54] billion USD (Fig. 4).

Based on a continuation of the historical trend pathway SSP2 and limiting the global warming to 2.0 °C scenario, the estimated annual drought loss will increase to 75 [95% confidence interval: 68–84] billion USD, which amounts to 0.21% of the projected national GDP of the corresponding period. In a strongly fragmented world SSP3 and the 2.0 °C target, drought loss will be about 61 [95% confidence interval: 56–68] billion USD, accounting for ∼0.21% of the GDP. In a growth-oriented world

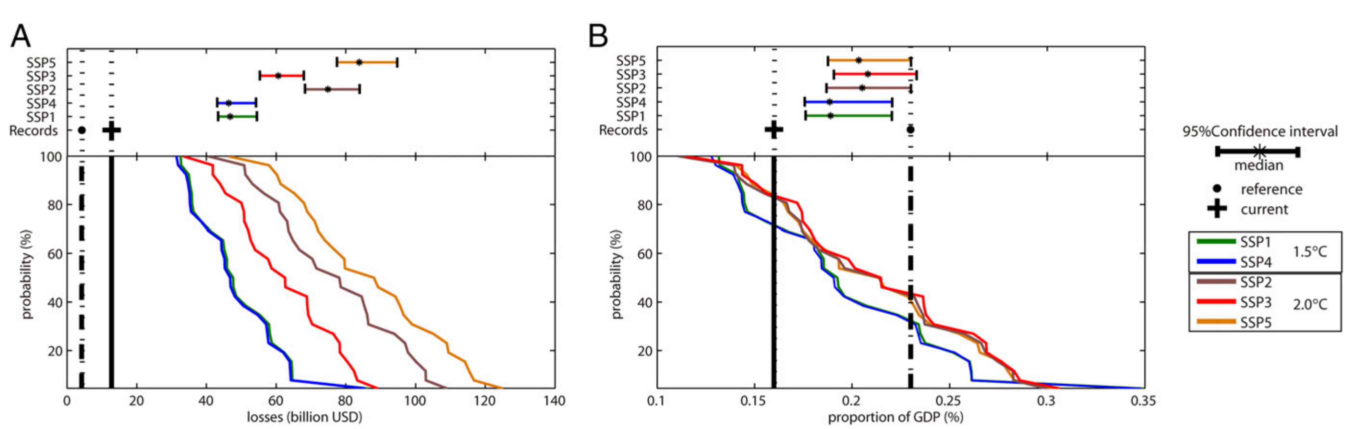

Fig. 4. Drought losses (*A*) and their share of GDP (*B*) at the global warming 1.5 °C and 2.0 °C levels under SSPs in China. Probability in vertical axis represents percentage of results exceeding a given loss (*A*) or given loss' share of GDP (*B*) of 44 combinations of 22 GCMs and two drought indices. Dotted black lines denote the recorded annual mean losses and their share of GDP in reference period and current status. Confidence intervals (95%) of projected losses and their share of GDP are shown for different SSPs. Asterisk is the multimodel median.

SSP5 of 2.0 °C, average drought loss is estimated to reach about 84 [95% confidence interval: 77–95] billion USD per year. This high figure reflects only 0.20% of the projected national GDP, due to the strong increase in the projected national GDP within SSP5. The annual average drought loss for the 2.0 °C warming level under the SSP5 is estimated to be 20 times of that in the reference period 1986–2005 and 1.8 times of that in the 1.5 °C warming level under SSP1 or SSP4, respectively (Fig. 4).

With increasing drought hazards and expected economic development across China, drought losses are projected to reach more than 80 billion USD, being higher by more than 30 billion USD in the 2.0 °C warming scenario under the growth-oriented world of SSP5 compared with that of 47 billion in the 1.5 °C warming scenario under the SSP1. Annual growth of GDP under pathways SSP1 and SSP5 are projected to be around 773 and 656 billion USD, respectively (*SI Appendix*, Fig. S7). That is, nearly 6.1% of the increase of GDP per year in the 1.5 °C warming world might be offset by drought losses, and the percent will increase to 12.8% in the 2.0 °C warming world.

Discussion and Conclusions

To evaluate climatic drought, many indices have been developed to describe variation of dry and wet episodes. The SPEI is designed to compare the evaporative demand by the atmosphere with the water availability, while the PDSI tried to represent the true water balance of the soils (19). Findings from the PDSI in our study are in line with regional results from a global-scale study by Sheffield et al. (28), who applied PDSI_PM that takes into account changes in available energy, humidity, and wind speed as we did in our study, and results from Wang et al. (29), who applied soil moisture condition as an indicator. Since PDSI depends on the current water availability, drought conditions assessed by the PDSI are less severe than the SPEI. Droughts in 1984–2015 in China, characterized by the PDSI, show a nonsignificant aggravation trend, but a significant dryness trend is detected by the SPEI (*SI Appendix*, Fig. S5). Especially in arid and semiarid climate regions, where annual precipitation is below 400 mm with a vast of area even less than 200 mm, a dryness trend is detected by the SPEI, but a weak wetting trend is found when the PDSI is examined. Note that the correlation between the PDSI and drought losses is found to be nonsignificant in arid and semiarid climate regions in China (*SI Appendix*, Fig. S5 and Table S5).

Besides for the SPEI and PDSI, which are widely used for agro-climatological analysis (18, 30), precipitation-based meteorological index SPI is often used to monitor moisture supply conditions (31). Comparison of time series of SPEI, PDSI, and SPI in China with that of recorded drought losses for 1984–2015 proves that variation of SPEI related closely to the changes of drought losses. A weak correlation between the SPI and drought losses means that not only precipitation but also evapotranspiration and soil moisture play major roles in regional drought development. However, biases in estimation of potential evapotranspiration (PET) under anthropogenic climate change could cause overestimation of drying trends (32, 33). Comparison with the evapotranspiration directly from the climate models at nonwater-stressed condition shows that Penman-Monteith–based analysis is a fair PET estimation method for studying droughts over all of China (*SI Appendix*, Tables S2 and S3).

Under the 1.5 °C global warming scenario, increasing trends of evapotranspiration and precipitation are projected in entire China, but a consistent drying trend is estimated both by SPEI and PDSI mainly in southern China and parts of Northwest China. A few regions in Northeast, North, and Southwest China show trends toward wetter conditions, caused by a stronger impact of increases in precipitation than in evapotranspiration. For an additional 0.5 °C global temperature increase, further intensification of droughts is projected in parts of East, Central, South, Northwest, and Southwest China, with a more pronounced rise in evapotranspiration, leading to more severe dryness conditions (Fig. 1). Considering that the sensitivities of these indices to climate change are different, drought conditions for the 1.5 °C and the 2.0 °C warming levels, deduced by SPI, are also projected to clarify the differences. According to the SPI, averaged coverage and frequency of drought events will decrease due to the increased precipitation in the warming world, but drought intensity is projected to increase for the 1.5 °C and 2.0 °C levels relative to the reference period (*SI Appendix*, Fig. S11).

It becomes clear that absolute drought losses in China will increase under every projected socioeconomic pathway. Along with rapid growth of the socioeconomic conditions, drought losses by the SPI will more than double the observational records in the warming world, but being obviously lower than by other two indices. By the SPEI and PDSI, drought losses will more than triple the records, with more losses for the 2.0 °C target than for the 1.5 °C (*SI Appendix*, Fig. S13 and Tables S6 and S7). The huge increase of losses from droughts by the SPEI and PDSI is due largely to rapid development of future economy, but still attributable to the projected regional dryness trend. Drought losses in the warming climate, for the 1.5 °C and 2.0 °C warming levels, under the assumption of fixed GDP at the year 2010 level, are projected to be, respectively, 48–52% and 58–70% higher than for the recent interval of 2006–2015 (*SI Appendix*, Table S8).

In relation to loss share on the national GDP, a significant decreasing trend was recorded in the recent decades from 0.23% in 1986–2005 to 0.16% in 2006–2015 due to the rapid increase of national GDP. However, the trend was projected to reverse in the future, with this share gradually increasing under the warming climate and possibly approaching the level of the reference period in the 2.0 °C scenario, taking improved adaptation capacity into account. Keeping the increase in global average temperature less than or equal to the 1.5 °C above the preindustrial level can reduce the drought losses almost twofold in China, by several tens of billions of USD (*SI Appendix*, Table S6). Case of drought risks in China presents a clear argument to focus efforts on mitigation, so that the 1.5 °C warming limit is not exceeded.

Data and Methods

Climatic and Socioeconomic Data. Climate projections are based on available ensemble runs by GCMs from CMIP5 (*SI Appendix*, Table S1). Altogether 22 simulations from 13 models, namely GFDL-ESM2M, HadGEM2-ES, IPSL-CM5A-LR, NorESM1-M, CNRM-CM5, MIROC-ESM-CHEM, CanESM2, GFDL-CM3, GFDL-ESM2G, IPSL-CM5A-MR, MIROC-ESM, MIROC5, and MRI-CGCM3, are found to meet the research requirement for calculation of potential evapotranspiration for historical period and future period under RCP2.6 and RCP4.5 scenarios. The GCM outputs were bias-corrected, based on observational data by Equidistant Cumulative Distribution Functions (EDCDF) method and downscaled statistically to a regular geographical grid with a 0.5° resolution by the spatial disaggregation (SD) method. The bias correction and statistical downscaling lead to an improvement of GCMs in reproducing the observed spatial pattern and long-term average of climatic variables (*SI Appendix*, Figs. S2–S4), and thus, intensity of drought events can be also well captured by GCMs (*SI Appendix*, Fig. S6).

Observational gridded dataset of climate variables (daily precipitation, temperature, relative humidity, wind speed, shortwave radiation estimated by the sunshine duration) with 0.5° resolution used as a reference in the downscaling method is constructed in the National Climate Center of China Meteorological Administration based on nearly 2,400 ground-based stations in China by means of the "anomaly approach" method (34).

County-level socioeconomic data for 1984–2015 in China stem from the China Statistical Yearbook (35). The data are interpolated into a geographical grid corresponding to the 0.5° resolution of the GCM's outputs using the area-weighted interpolation method. Provincial scale GDP in China under SSPs for 2010–2060 is projected by Cobb–Douglas production model with regionalized parameters, including labor force, total factor productivity, and capital stock. The latest universal two-child policy in China is fully considered for labor force projection, and initial information on fertility, deaths, migration, total factor productivity, and capital stock, are from the latest demographical and economic census. The parameterization scheme for SSP1–5 is followed in refs. 12 and 36. To maintain the homogeneity of the data series, GDPs recorded in 1986–2015 and projected in 2010–2060 are standardized to 2015 prices (*SI Appendix*, Fig. S7). Gridded GDP for the period 2010–2060 is derived by scaling the provincial GDP projections to 0.5° resolution, based on the weights of individual grid cells to the entire provincial GDP, which are deduced from the observational period (37).

Droughts and their direct economic losses are recorded once an event with coverage ≥50,000 km^2 and duration ≥20 d happened in any province from 1984 to 2015 (24). The datasets are checked and ratified by Ministry of Civil Affairs and National Committee for Disaster Reduction in China with data from several sectors, including China Meteorological Administration, Ministry of Agriculture, Ministry of Water Resources, and National Bureau of Statistics.

Identification of Drought Events. Drought events are identified according to the SPEI, PDSI, SPI, and the cluster analysis method. The SPEI approach proposed in ref. 18 is the standardization of the difference between precipitation and potential evapotranspiration, while the SPI developed in ref. 31 is used to quantify the precipitation deficits or surpluses only. The self-calibrated PDSI (20, 21) is based on the supply and demand model of soil moisture. In this study, potential evapotranspiration in both the SPEI and PDSI is deduced with the Penman–Monteith equation (38), as recommended by the Food and Agriculture Organization (FAO). Available water holding capacity required for the PDSI actual evapotranspiration is provided by the Potsdam Institute for Climate Impact Research using the FAO digitized soil map (39). For detailed information on the way of potential and actual evapotranspiration calculation, see *SI Appendix*, SI2. Parameters included in calculation process of the drought indices are estimated in the reference period and then used in the future to make sure that the dryness or wetness conditions in the warming levels are based on the status in the reference period.

Drought indices are calculated for a monthly time scale at each grid. Dryness is diagnosed once SPEI ≤ -1, PDSI ≤ -2 or SPI ≤ -1, and the lower the value of SPEI, PDSI, or SPI, the more severe the dryness condition (*SI Appendix*, Table S4). A cluster analysis method is used to identify the drought events (8, 22, 40, 41) by determining the drought center (grid with maximum intensity) first and then clustering all neighboring grid cells that fit the drought criteria of SPEI ≤ -1, PDSI ≤ -2, or SPI ≤ -1. Summed area of clustered grids is the areal coverage of a drought event, and averaged value of drought indices over the summed area is the intensity of a drought event (*SI Appendix*, SI3). As the drought events and losses recorded in the meteorological disaster yearbook of China only refer to events covering an area larger than 50,000 km^2, drought events of a smaller spatial scale are not considered in this study.

Intensity-Loss Rate Function. To estimate the losses caused by drought events of different intensities, the intensity-loss rate curves are set up for each province in China based on the direct economic losses of droughts during the period 1984–2015, which are recorded in the yearbook of meteorological disasters in China (24). For each province, the drought intensity is averaged for all drought events per year. The loss rate is the ratio between annual drought losses and GDP in drought areal coverage in a province. For reflecting the improved adaptation capacity to cope with meteorological disaster in the future, the slope of the intensity-loss rate curve is designed to change together with socioeconomic condition (*SI Appendix*, SI6). The intensity-loss rate, combined with future drought exposure and projected drought intensity, is used for the estimation of future drought losses.

ACKNOWLEDGMENTS. We thank the World Climate Research Programme's working group on coupled modeling for producing and making available their model output, and the constructive advice of Dr. P. C. D. Milly is gratefully acknowledged. This study is jointly supported by National Key R&D Program of China Grant 2017YFA0603701, National 1000 Talent Program Grant Y474171, and National Natural Science foundation of China Grants 41671211 and 41661144027.

1. Handmer J, et al. (2012) Changes in impacts of climate extremes: Human systems and ecosystems. *Managing the Risks of Extreme Events and Disasters to Advance Climate Change Adaptation. A Special Report of Working Groups I and II of the Intergovernmental Panel on Climate Change (IPCC)*, eds Field CB, et al. (Cambridge Univ Press, Cambridge, UK), pp 231–290.
2. EM-DAT (2017) EM-DAT: The OFDA/CRED international disaster database (Univ Catholique de Louvain, Brussels). Available at https://www.emdat.be. Accessed September 15, 2018.
3. Dai A (2013) Increasing drought under global warming in observations and models. *Nat Clim Change* 3:52–58.
4. Trenberth KE, et al. (2014) Global warming and changes in drought. *Nat Clim Change* 4:17–22.
5. Dai A, Zhao T (2016) Uncertainties in historical changes and future projections of drought. Part I: Estimates of historical drought changes. *Clim Change* 144:519–533.
6. Fischer T, Gemmer M, Liu L, Su BD (2011) Temperature and precipitation trends and dryness/wetness pattern in the Zhujiang River Basin, South China, 1961-2007. *Quat Int* 244:138–148.
7. Chen HP, Sun JQ (2015) Changes in drought characteristics over China using the standardized precipitation evapotranspiration index. *J Clim* 28:5430–5447.
8. Zhai JQ, et al. (2017) Intensity- area-duration analysis of droughts in China 1960-2013. *Clim Dyn* 48:151–168.
9. Sheffield J, Wood EF (2008) Projected changes in drought occurrence under future global warming from multi-model, multi-scenario, IPCC AR4 simulations. *Clim Dyn* 31:79–105.
10. UNFCCC (United Nations Framework Convention on Climate Change) (2015) Report of the ad hoc working group on the Durban platform for enhanced action on the eighth part of its second session, held in Geneva from 8 to 13 February 2015 (United Nations, Geneva), Technical Report FCCC/ADP/2015/2.
11. IPCC (Intergovernmental Panel on Climate Change) (2013) *Summary for Policymakers. Climate Change 2013: The Physical Science Basis. Contribution of Working Group I to the Fifth Assessment Report of the Intergovernmental Panel on Climate Change*, eds Stocker TF, et al. (Cambridge Univ Press, Cambridge, UK).
12. Leimbach M, Kriegler E, Roming N, Schwanitz J (2017) Future growth patterns of world regions–A GDP scenario approach. *Glob Environ Change* 42:215–225.
13. Warszawski L, et al. (2014) The inter-sectoral impact model intercomparison project (ISI–MIP): Project framework. *Proc Natl Acad Sci USA* 111:3228–3232.
14. Burke EJ, Brown SJ (2008) Evaluating uncertainties in the projection of future drought. *J Hydrometeorol* 9:292–299.
15. Orlowsky B, Seneviratne SI (2013) Elusive drought: Uncertainty in observed trends and short- and long-term CMIP5 projections. *Hydrol Earth Syst Sci* 17:1765–1781.
16. Touma D, Ashfaq M, Nayak MA, Kao SC, Diffenbaugh NS (2015) A multi-model and multi-index evaluation of drought characteristics in the 21st century. *J Hydrol* 526:196–207.
17. Sun QH, Moa CY, Duan QY (2015) Projected changes in temperature and precipitation in ten river basins over China in 21st century. *Int J Climatol* 35:1125–1141.
18. Vicente-Serrano SM, Beguería S, Lopez-Moreno JI (2010) A multiscalar drought index sensitive to global warming: The standardized precipitation evapotranspiration index. *J Clim* 23:1696–1718.
19. Beguería S, Vicente-Serrano SM, Reig F, Latorre B (2014) Standardized precipitation evapotranspiration index (SPEI) revisited: Parameter fitting, evapotranspiration models, tools, datasets and drought monitoring. *Int J Climatol* 34:3001–3023.
20. Palmer WC (1965) Meteorological drought, U.S. Weather Bureau Research Paper No. 45 (US Government Printing Office, Washington, DC).
21. Wells N, Goddard S (2004) A self-calibrating palmer drought severity index. *J Clim* 17: 2335–2351.
22. Sheffield J, Andreadis KM, Wood EF, Lettenmaier DP (2009) Global and continental drought in the second half of the twentieth century: Severity-area-duration analysis and temporal variability of large scale events. *J Clim* 22:1962–1981.
23. Xu K, et al. (2015) Spatio-temporal variation of drought in China during 1961-2012: A climatic perspective. *J Hydrol* 526:253–264.
24. China Meteorological Administration (2016) *Yearbook of Meteorological Disasters in China* (China Meteorolog Press, Beijing).
25. Hirabayashi Y, et al. (2013) Global flood risk under climate change. *Nat Clim Change* 3:816–821.
26. O'Neill BC, et al. (2017) The roads ahead: Narratives for shared socioeconomic pathways describing world futures in the 21st century. *Glob Environ Change* 42:169–180.
27. van Vuuren DP, et al. (2014) A new scenario framework for climate change research: Scenario matrix architecture. *Clim Change* 122:373–386.
28. Sheffield J, Wood EF, Roderick ML (2012) Little change in global drought over the past 60 years. *Nature* 491:435–438.
29. Wang AH, Lettenmaier DP, Sheffield J (2011) Soil moisture drought in China, 1950-2006. *J Clim* 24:3257–3271.
30. Alley WM (1984) The Palmer drought severity index: Limitations and assumptions. *J Clim Appl Meteorol* 23:1100–1109.
31. McKee TB, Doesken NJ, Kleist J (1993) The relationship of drought frequency and duration to time scales. *Proceedings of the Eighth Conference on Applied Climatology* (Am Meteorolog Soc, Boston), pp 179–184.
32. Milly PCD, Dunne A (2017) A hydrologic drying bias in water-resource impact analyses of anthropogenic climate change. *J Am Water Resour Assoc* 53:822–838.
33. Milly PCD, Dunne A (2016) Potential evapotranspiration and continental drying. *Nat Clim Change* 6:946–950.
34. Wu J, Gao XJ (2013) A gridded daily observation dataset over China region and comparison with the other datasets. *Chin J Geophys* 56:1102–1111.
35. National Bureau of Statistics of China (2016) *China Statistical Yearbook 2015* (China Stat Press, Beijing).
36. Kc S, Lutz W (2017) The human core of the shared socioeconomic pathways: Population scenarios by age, sex and level of education for all countries to 2100. *Glob Environ Change* 42:181–192.
37. Jiang T, et al. (2018) National and provincial economic change projected to 2100 under the Shared Socioeconomic Pathways in China. *Adv Clim Chang Res* 14:50–58.
38. Allen RG, Pereira LS, Raes D, Smith M (1998) *Crop Evapotranspiration–Guidelines for Computing Crop Water Requirements–FAO Irrigation and Drainage Paper 56* (Food and Agric Org, Rome).
39. FAO (1991) *The Digitized Soil Map of the World (Release 1.0)* (Food and Agric Org, Rome).
40. Andreadis KM, Clark EA, Wood AW, Hamlet AF, Lettenmaier DP (2005) Twentieth-century drought in the conterminous United States. *J Hydrometeorol* 6:85–101.
41. Huang JL, et al. (2017) Analysis of future drought characteristics in China using the regional climate model CCLM. *Clim Dyn* 50:507–525.